

Molecular Crystals and Liquid Crystals Science and Technology. Section A. Molecular Crystals and Liquid Crystals

Publication details, including instructions for authors and subscription information:

<http://www.tandfonline.com/loi/gmcl19>

Structural Properties of the Ferroelectric Liquid Crystal Mixtures Based on the Homologous Series of Alkoxyphenyl Alkoxy Benzoates

D. Ž. Obadović^a, L. Bata^b, T. Tóth-Katona^b, A. Bóta^c, K. Fodor-csorba^b, A. Vajda^b & M. Stančić^d

^a Institute of Physics, Faculty of Sciences, Trg D. Obradovića 4, Novi Sad, Yugoslavia

^b Res. Inst. for Solid State Physics of the Hungarian Academy of Sciences, P. O. B. 49, H-1525, Budapest, Hungary

^c Technical University, Budapest, Hungary

^d Technical Faculty "Mihajlo Pupin", Zrenjanin, Yugoslavia

Version of record first published: 04 Oct 2006

To cite this article: D. Ž. Obadović, L. Bata, T. Tóth-Katona, A. Bóta, K. Fodor-csorba, A. Vajda & M. Stančić (1997): Structural Properties of the Ferroelectric Liquid Crystal Mixtures Based on the Homologous Series of Alkoxyphenyl Alkoxy Benzoates, *Molecular Crystals and Liquid Crystals Science and Technology. Section A. Molecular Crystals and Liquid Crystals*, 303:1, 85-96

To link to this article: <http://dx.doi.org/10.1080/10587259708039410>

PLEASE SCROLL DOWN FOR ARTICLE

Full terms and conditions of use: <http://www.tandfonline.com/page/terms-and-conditions>

This article may be used for research, teaching, and private study purposes. Any substantial or systematic reproduction, redistribution, reselling, loan, sub-licensing, systematic supply, or distribution in any form to anyone is expressly forbidden.

The publisher does not give any warranty express or implied or make any representation that the contents will be complete or accurate or up to date. The accuracy of any instructions, formulae, and drug doses should be independently verified with primary sources. The publisher shall not be liable for any loss, actions, claims, proceedings, demand, or costs or

damages whatsoever or howsoever caused arising directly or indirectly in connection with or arising out of the use of this material.

STRUCTURAL PROPERTIES OF THE FERROELECTRIC LIQUID CRYSTAL MIXTURES BASED ON THE HOMOLOGOUS SERIES OF ALKOXYPHENYL ALKOXY BENZOATES

D. Ž. Obadović*, L. Bata, T. Tóth-Katona, A. Bóta**, K. Fodor-Csorba, A. Vajda and M. Stančić***

* Institute of Physics, Faculty of Sciences, Trg D. Obradovića 4, Novi Sad, Yugoslavia

Res. Inst. for Solid State Physics of the Hungarian Academy of Sciences, H - 1525 Budapest, P.O.B. 49, Hungary

** Technical University, Budapest, Hungary

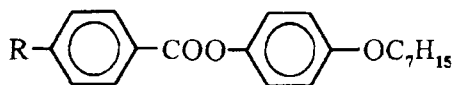
*** Technical Faculty "Mihajlo Pupin", Zrenjanin, Yugoslavia

Abstract The temperature dependence of the layer spacings and the average intermolecular distances were studied in smectic *A*, *C*, *B* and nematic phases by X-ray diffraction on non-oriented samples. Two representatives of 4-*n*-alkoxyphenyl 4'-*n*-alkoxy benzoates, furthermore their eutectic binary mixture, and ternary ferroelectric mixtures obtained by the chiral additive of (R)-(1-methylheptyl)-1,1'-4'-1"-terphenyl-1,4"-dicarboxylate used in different concentrations were investigated by small and large angle measurements as well.

INTRODUCTION

Recently much efforts have been paid to get ferroelectric mixtures for display devices.¹ In these mixtures smectic C (*SmC*), smectic A (*SmA*), nematic (*N*), isotropic (*I*) phase sequence is preferable.

The binary mixture (*Mix.1*) of 4'-*n*-heptyloxy-phenyl-4-*n*-octyloxy benzoate (*Comp.1*) and 4'-*n*-heptyloxy-phenyl-4-*n*-decyloxy benzoate (*Comp.2*)² has *SmC* phase in a wide temperature range (see molecular structure and Table I).



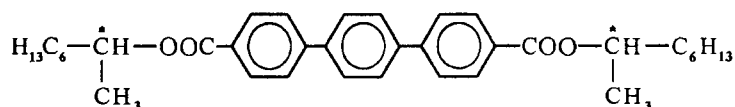
R=C₈H₁₇O- *Comp.1*, R=C₁₀H₂₁O- *Comp.2*

TABLE I The phase sequences of the investigated substances.

Subst.	Phase sequence (in °C)	Concentration (wt%)		
		<i>Comp.1</i>	<i>Comp.2</i>	<i>Comp.3</i>
<i>Comp.1</i>	<i>Cr</i> 62 <i>SmC</i> 69 <i>N</i> 88 <i>I</i>	100	–	–
<i>Comp.2</i>	<i>Cr</i> 67 <i>SmC</i> 79 <i>SmA</i> 82 <i>N</i> 89 <i>I</i>	–	100	–
<i>Comp.3</i>	<i>Cr</i> 82 <i>I</i>	–	–	100
<i>Mix.1</i>	<i>Cr</i> 51 (<i>SmB</i> 33) <i>SmC</i> 76 <i>SmA</i> 78 <i>N</i> 89 <i>I</i>	50	50	–
<i>Mix.2</i>	<i>Cr</i> 48 <i>SmC</i> * 73 <i>SmA</i> * 75 <i>N</i> * 79 <i>I</i>	38.4	38.4	23.2
<i>Mix.3</i>	<i>Cr</i> 52 <i>SmC</i> * 73 <i>SmA</i> * 77 <i>N</i> * 88 <i>I</i>	46.1	46.1	7.8

In our previous study³ we have observed monotropic smectic *B* (*SmB*) phase below *SmC* only in this binary mixture *Mix.1*, however none of the compounds *Comp.1* and *Comp.2* exhibited this highly ordered smectic phase (Table I).

Chiral additive, *bis-(R)-(1-methylheptyl)-1,1'-4'-1''-terphenyl-1,4''-dicarboxylate* (*Comp.3*)⁴:



do not have any liquid crystalline phases (see Table I). The addition of this compound to the *Mix.1* in different concentrations results in formation of the ferroelectric liquid crystal mixtures (*Mix.2* and *Mix.3*).³ The phase sequences of these ternary mixtures can be also seen in Table I, which shows that *Comp.3* has stabilizing effect on *SmC** phase.

Some physical and electro-optical properties of the compounds as well as their binary and ternary mixtures: phase diagrams, spontaneous polarization, tilt angle and switching time have been studied previously.³ *Mix.2* exhibited spontaneous polarization of about $\approx 200\text{nC/cm}^2$ and switching time of $\approx 0.3\text{ms}$. This phenomenon initiated the more detailed structural studies of these mixtures by X-ray diffraction method. The layer spacing (*d*), and the average intermolecular distance (*D*) i.e. the mean distance between long axes of neighbouring parallel molecules were determined using the Bragg law: $\lambda = 2x\sin\Theta$, where distances $x = d$ and $x = D$ were calculated from the position of the small angle and large angle diffraction peak, respectively.

EXPERIMENTAL

Optical studies of the textures, the phase transition temperature measurements, and the miscibility studies were carried out with an Amplival pol-u polarizing microscope equipped with a Boetius hot-stage. The investigations were done in non-oriented sandwich cells with the crossed polarizers of the microscope.

For the small angle X-ray (SAX) measurements the samples were transferred into thin-walled Mark quartz-capillaries (Hilgenberg, Germany) of 1 mm. The capillaries were closed with two component synthetic resin and transferred in metal capillary holders into a home-built aluminium block. This block was settled in the beamline directly and used as a thermal gradient incubator for temperature control. The block was held at the desired temperatures by thermostat. The actual temperatures were constant to within less than 0.05°C as controlled by a thermocouple. The windows of the block were covered with Mylar foil.

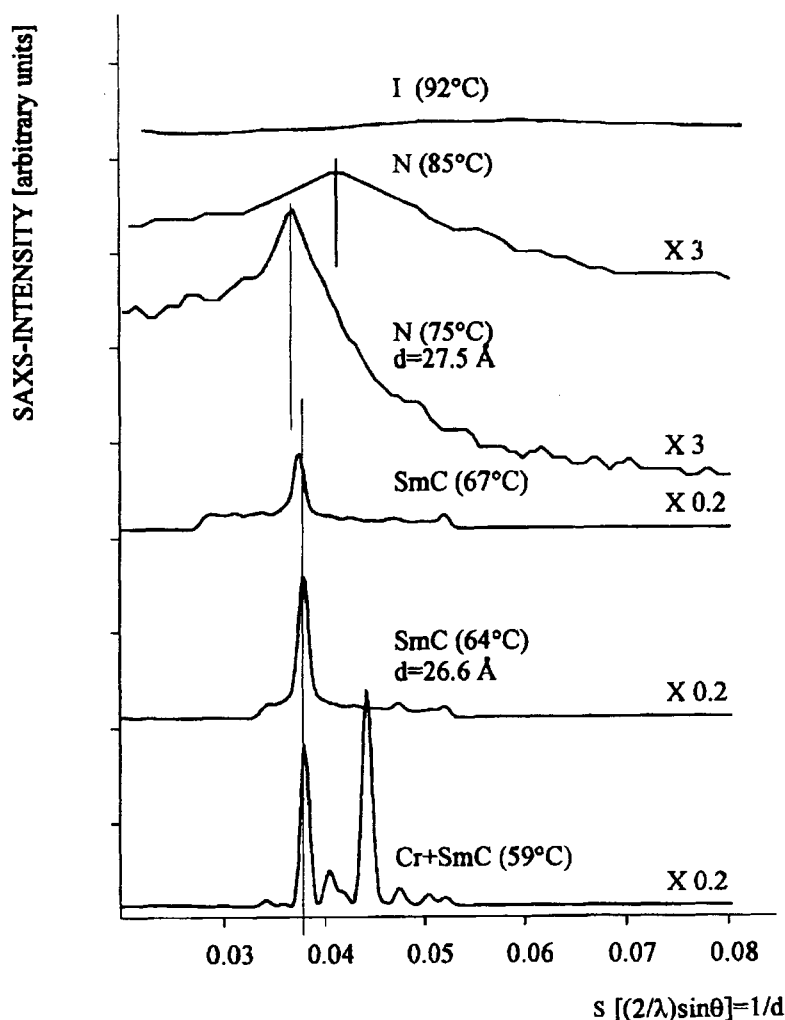
The SAX camera was a Kratky camera (Anton Paar, Graz, Austria) attached to the line-focus window of a Cu-tube at a generator (Seifert, Ahrensburg, Germany) operated at 40 kV and 20 mA. A Ni-filter was used to eliminate K_{β} radiation. The scattering data were collected with a proportional counter. The scattering data curves were normalized and desmeared for the slit geometry.

The large angle X-ray diffraction studies were made on unoriented samples in a transmission geometry by means of a conventional power diffractometers. For the determination of the intermolecular distance D , the Seifert V-14, CuK_{α} radiation at 0.154nm was used with an automatical high temperature kit Paar HTK-10.

RESULTS

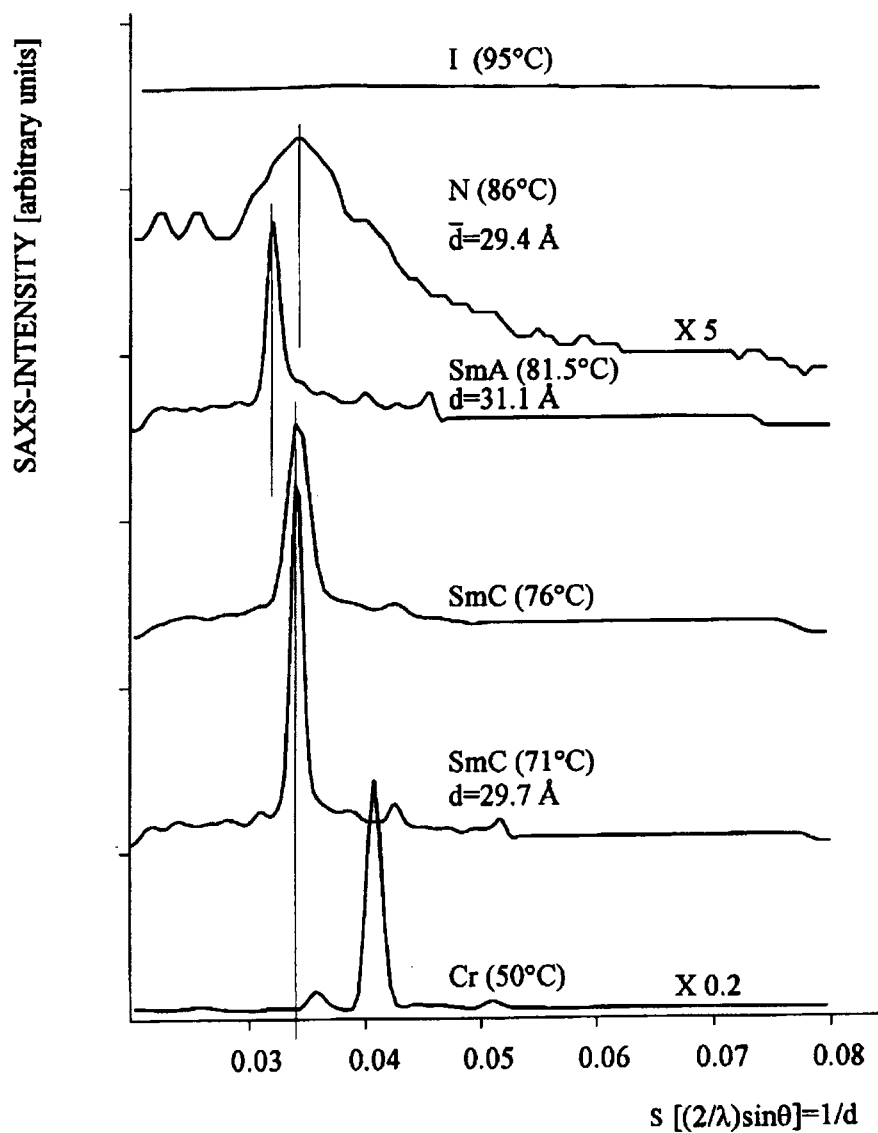
X-Ray Diffraction Studies on Single Components of the Liquid Crystalline Mixtures

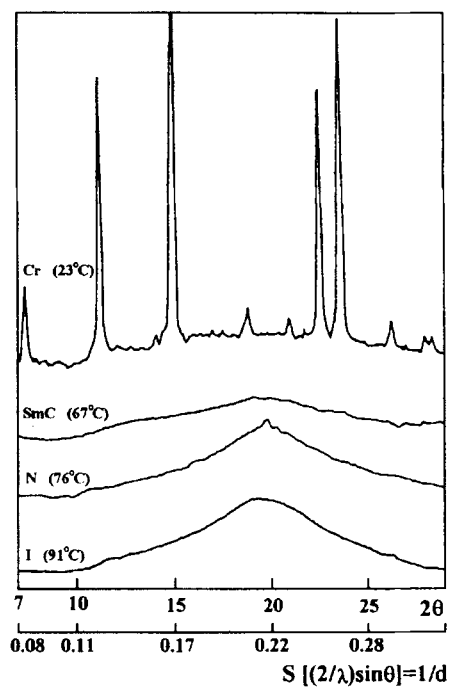
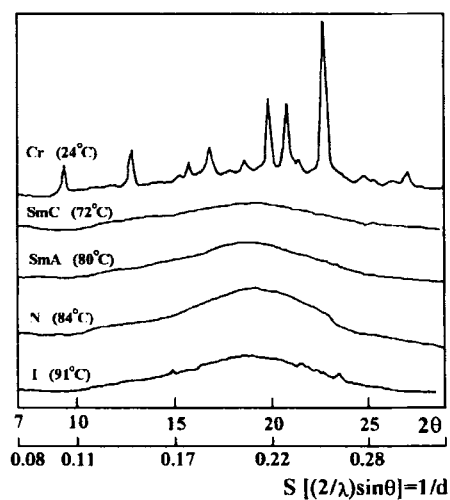
X-ray diffraction studies were carried out on the single components of liquid crystal mixtures in all the phases they exhibited. Diffraction profiles of a non-oriented samples of *Comp.1* and *Comp.2* at different temperatures are given at Figures 1, 2 and 3, 4, both for small and large diffraction angles. The analysis of X-ray diagrams of *SmC* phase shows the presence of a strong reflections at small angles, indicating the layer structure, and the diffuse outer scattering corresponds to average intermolecular distance D . The calculation of effective layer thickness d , gives the value of 26.6\AA and 29.7\AA for *Comp.1* and *Comp.2*, respectively. Smectic *SmA* phase appearing at 81.5°C in the case of *Comp.2*, is characterized by the small angle diffraction line and by the broad diffuse peak at larger angles (Figures 2 and 4, respectively). The first one is characterized by the width of smectic layers $d = 31.1\text{\AA}$ and the other one by the intermolecular distance $D = 5.15\text{\AA}$. It was concluded that with temperature rise the distance between long axes of the neighbouring parallel molecules increases and in the case of sample *Comp.2* D is larger than for *Comp.1* (Figure 5.a and b). This indicates that the deviation from the extended conformation of the molecule with longer polymethylene chain ($d(\text{Comp.2}) > d(\text{Comp.1})$) is larger, which contributes to smaller packing density of the molecules along the layer.

FIGURE 1: X-ray diffraction profiles at small angles for *Comp.1*.

Diffraction spectrum of the nematic phase corresponds to the spectrum of classical uniaxial nematics containing two liquid-like X-ray diffraction maxima, one corresponding to the mean repeat distance along the director axis $d = 27.5\text{Å}$ and 29.4Å , for *Comp.1* and *Comp.2*, respectively, and the other one corresponding to the mean lateral intermolecular spacing, giving the value $D = 5.15\text{Å}$ and 5.35Å for *Comp.1* and *Comp.2*, respectively.

In order to get additional information, the molecular lengths (l) for *Comp.1* and *Comp.2* have been also determined by calotte model in all-trans conformation and values of $l = 34.3\text{Å}$ and $l = 36.2\text{Å}$ were found, respectively.

FIGURE 2: X-ray diffraction profiles at small angles for *Comp.2*.

FIGURE 3: X-ray diffraction profiles at large angles for *Comp.1*.FIGURE 4: X-ray diffraction profiles at large angles for *Comp.2*.

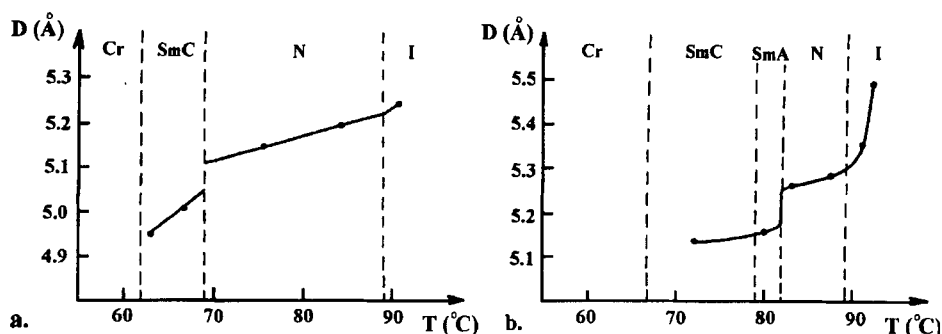


FIGURE 5: Plots of D versus temperature T for a. *Comp.1*, and b. *Comp.2*.

X-Ray diffraction studies of the Liquid Crystalline Mixtures

It was found on the basis of optical microscopy data that eutectic mixture of *Comp.1* and *Comp.2* (*Mix.1*) includes *SmC* and *SmA* phase, as well as the *N* phase, both on heating and cooling, while *SmB* phase appears only during the cooling process, showing monotropic transition at 33°C .³

In the binary mixture *Mix.1* diffraction pattern at large angles (Figure 6) shows a continuous decrease in the angular dependence of the diffuse peak with temperature rise, which corresponds to the increase of the lateral intermolecular distance D .

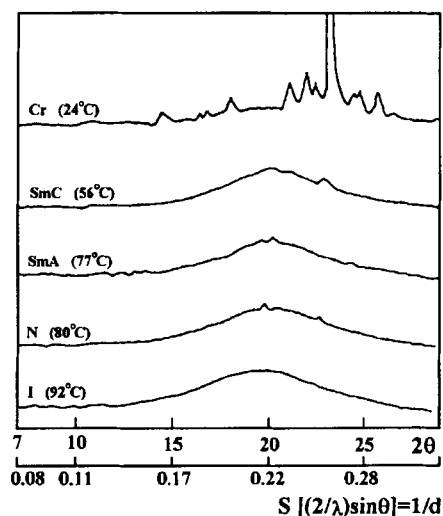


FIGURE 6: X-ray diffraction profiles at large angles for binary mixture *Mix.1*.

In the *SmC* phase of binary mixture *Mix.1* diffraction pattern at small angles (Figure 7.) shows the presence of two clearly pronounced peaks, where the first one characterizes the width of smectic layers $d = 28.4\text{Å}$ at $T = 72^\circ\text{C}$ and $d = 27.5\text{Å}$ at

$T = 56^\circ\text{C}$ – see Figure 6. During the transition to *SmA* phase, interlayer distance increases as the tilt angle decreases and becomes $d = 29.8\text{\AA}$ at $T = 78^\circ\text{C}$. Diffraction pattern of *SmB* phase reminds to the crystalline phase by its clearly expressed maximum at small angles ($d = 24.1\text{\AA}$), and well defined peaks superimposed to broad diffuse peak in the region $2\Theta = 15 - 27^\circ$. The higher temperature of the *SmB* phase detection (40°C – Figure 7) in comparison to the phase transition temperature obtained by polarization microscopy (33°C) is presumably due to the relatively high cooling rate applied in optical studies.

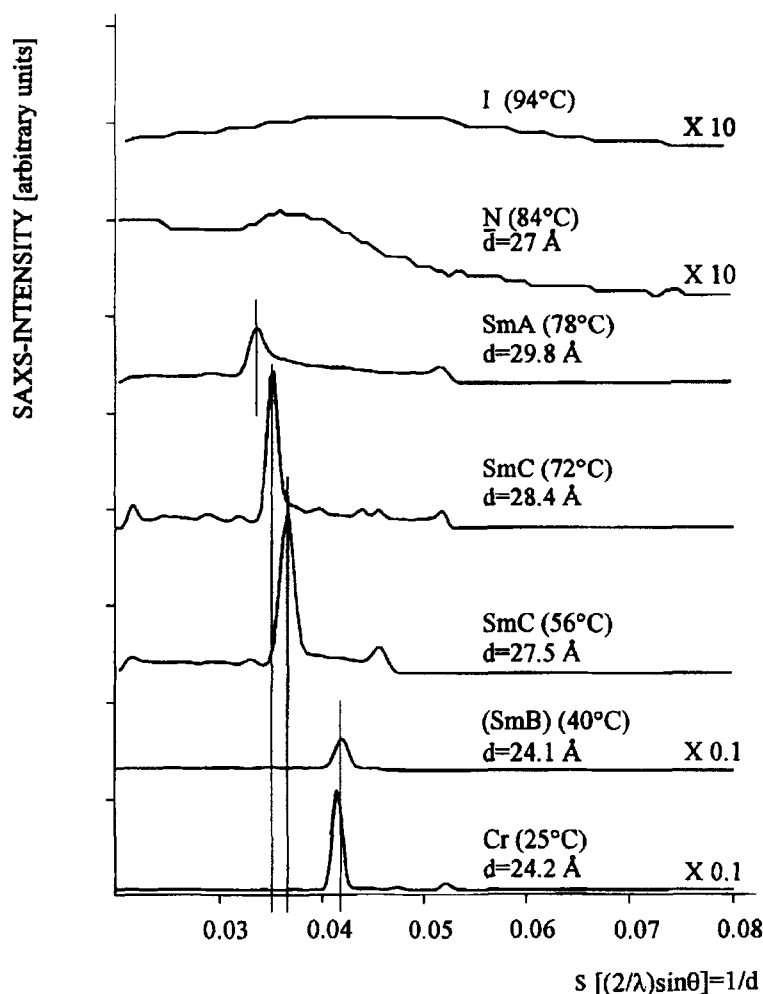


FIGURE 7: X-ray diffraction profiles at small angles for binary mixture *Mix.1*.

However, *Comp.3* has no liquid crystalline phase; the addition of it to the *Mix.1* leads to the formation of chiral mesophases in *Mix.2* and in *Mix.3*. Furthermore,

Comp.3 had a stabilizing effect on the SmA^* and on the SmC^* phase as well. The same chiral additive has shortened the N^* phase (compared to the temperature range of N phase in *Mix.1*) and caused the disappearance of the monotropic SmB phase.³

X-ray diffraction profiles of *Mix.2* at large angles (Figure 8) show decreament in the angular dependence of the diffuse outer peak with temperature rise, i.e., an increase of the average intermolecular distance D (Figure 9) similarly to the case of *Comp.1* and *Comp.2*.

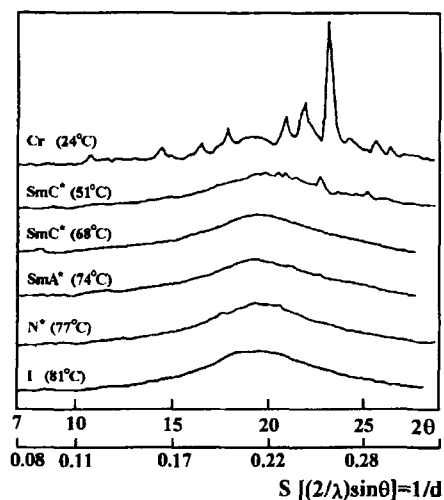


FIGURE 8: X-ray diffraction profiles at large angles for ternary mixture *Mix.2*.

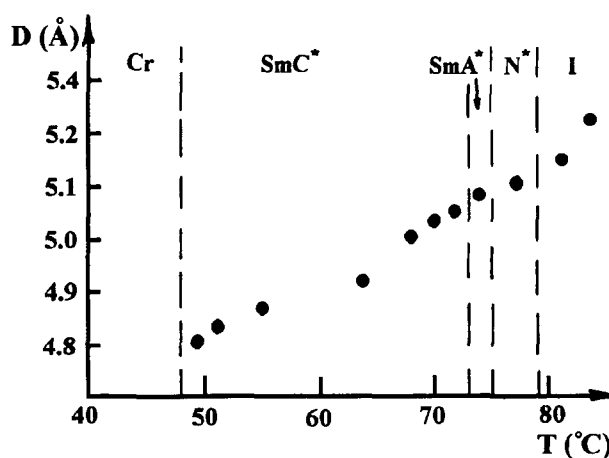


FIGURE 9: Plot of D versus temperature T for *Mix.2*.

The SmC^* phase of three-component mixture *Mix.3*, is characterized by an intensive peak at small angles, which shifts toward smaller angles θ with temperature rise (Figure 10). It means that the tilt angle ϑ is decreasing with temperature rise.

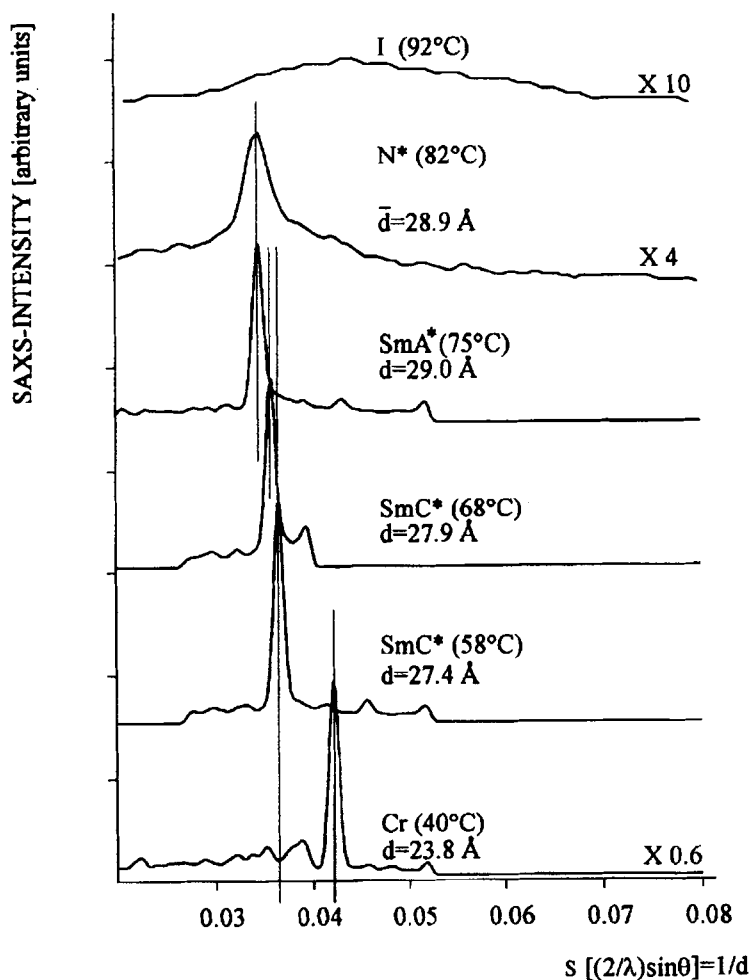


FIGURE 10: X-ray diffraction profiles at small angles for ternary mixture *Mix.3*.

The SmA phase is characterized by a single diffraction maximum at small angles, with corresponding interlayer distance $d = 29.0 \text{ \AA}$. During the transition into cholesteric and isotropic phase, the intensity of this maximum decreases and shifts towards larger angles (Figure 10), which indicates the decrease of the molecular length with the temperature rise.

From the large angle diffraction profiles of *Mix.3* (Figure 11) the similar temperature dependence of D can be obtained as for all the other investigated compounds or mixtures: D increases with temperature rise.

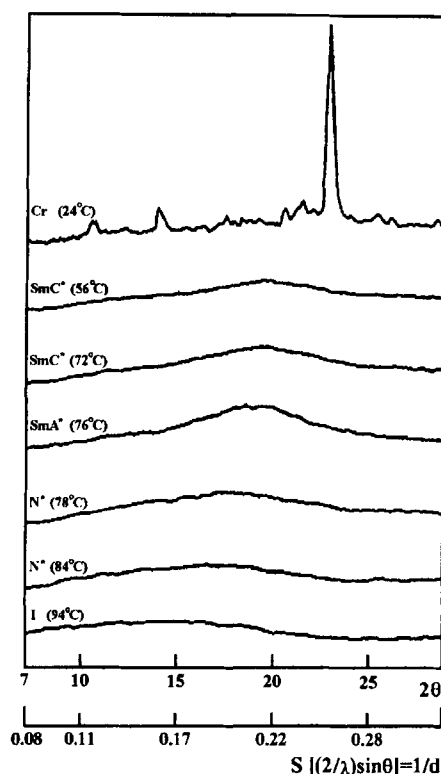


FIGURE 11: X-ray diffraction profiles at large angles for ternary mixture *Mix.3*.

CONCLUDING REMARKS

We have performed X-ray diffraction on the crystalline powder of unoriented samples of *Comp.1* and *Comp.2*, their eutectic mixture *Mix.1*, and ternary ferroelectric mixtures *Mix.2* and *Mix.3* obtained by adding the non liquid crystalline chiral additive *Comp.3* in different concentrations. On the basis of these results the molecular parameters were determined in all liquid crystalline phases. The tilt angle in SmC phase was calculated by the equation $\vartheta = \arccos \frac{d_C}{d_A}$ and we found values of $\vartheta = 19^\circ$ for *Comp.2*, $\vartheta = 22.6^\circ$ at 56°C and $\vartheta = 17.6^\circ$ at 72°C for *Mix.1*, and $\vartheta = 19.1^\circ$ at 58°C and $\vartheta = 15.8^\circ$ at 68°C for *Mix.3*.

An increase of the intermolecular distance D was detected for all the investigated substances with the rise of temperature, which is the result of the decrease of the packing density of the molecules perpendicular to the long axes. The molecular packing along the long axis is characterized by the distances in nematic phase (Figures 1, 2, 7 and 10). One can notice the decrease of the length of the molecule with the increase of the temperature in the nematic phase and it is presumably the

consequence of the deviation of the molecule from extended all-trans conformation which is larger if the length of the polymethylene chain is longer.

ACKNOWLEDGEMENT

T.T.K. is indebted to the Institute of Physics, Novi Sad for its kind hospitality. The work was financially supported by the Hungarian Academy of Sciences Grant No. OTKA T 014957, OTKA T 020905, OTKA T 016252 and by the Serbian Science Foundation Grant No. 01E18.

REFERENCES

1. R. Dabrowski, J. Szulc and B. Sosnovska, Mol. Cryst. Liq. Cryst., **215**, 13 (1991).
2. J.W. Goodby and T.M. Leslie, Liquid Crystals and Ordered Fluids (Plenum Press, New York, London, 1984), Vol. 4, p. 1.
3. A. Vajda, K. Fodor-Csorba, L. Bata, T. Paksi, Zs. Kakas, I. Jánossy and J. Hajtó, Mol. Cryst. Liq. Cryst., (in press).
4. M. Loseva, N. Chernova, A. Rabinovich, E. Pozhiadev, Yu. Narkevich, O. Petrashevich, E. Kazachkov, N. Korotkova, M. Schadt and R. Buchecker, Ferroelectrics, **114**, 357 (1991).